THE UNIVERSITY OF VERMONT

DEPARTMENT OF ELECTRICAL ENGINEERING

ANNUAL REPORT

(1 October 1973 to 30 September 1974)

Processing Electrophysiological Signals for the Monitoring of Alertness

Principal Investigator

David C. Lai

November 1974

Prepared under
Grant No.: NGR 46-001-041
for
Ames Research Center
National Aeronautics and Space Administration

TABLE OF CONTENTS

LIST OF FIGURES

Processing Electrophysiological Signals

for the Monitoring of Alertness

Abstract

This research project is concerned with the use of mathematical techniques for processing EEG signals associated with varying states of alertness. It requires the development and implementation of advanced signal modeling and data processing techniques; especially designed for the representation and prediction of bioelectric signals useful as estimators of states of alertness. In particular, our goal is to develop and implement efficient techniques for processing and modeling of EEG signals to extract the characteristics of signals associated with varying states of alertness. New representations for EEG signals which will enhance the features in estimating the states of alertness are sought after. Fast algorithms for implementing real-time computations of alertness estimates have also been developed. In this report, we present a new realization of the phase-distortionless digital filter which approaches real-time filtering and a new transform for EEG signals. This transform not only provides new information for the alertness estimates but also can be performed in real time. We are also developing a statistical test for stationarity in EEG signals. This test provides a method for determining the duration of the EEG signals necessary in estimating the short-time power or energy spectra for nonstationary analysis of EEG signals. It also helps in extracting the dynamic properties of the signal process.

Processing Electrophysiological Signals for the Monitoring of Alertness

I. Introduction

The goal of this project is to develop and implement advanced techniques for processing and modeling of EEG signals to extract the characteristics of signals associated with varying states of alertness. These techniques are especially designed for the representation and prediction of electrophysiological signals useful as estimators of states of alertness. The purpose of signal representation is to transform the data into a domain which is more convenient, for some reason, to the particular user or users or for further analysis; e.g., data reduction or the enhancement of alertness estimates may be one of these goals.

Fourier series or transform has proven useful in the analysis of EEG signals in that it enhances the characteristics of the rhythmatic activities in EEG signals. With the advent of fast-Fourier-transform algorithm, the use of the Fourier spectral analysis has been widespread. However, it requires that the signal be at least wide-sense stationary. Since the EEG signals manifests the subject's brain states, the statistical characteristics vary as the states of the subject change during the course of time. It is more natural to treat EEG signals as nonstationary processes as proposed or as treated in [1] [2]. The general approach is to use a short-time power or energy spectral analysis. The success of this approach depends on the signal process remaining stationary during the duration for which the spectrum is obtained. The quantitative determination of this duration is important for both the accuracy and the efficiency of this analysis. We have used a sensitive test which

will not only determine the time interval of the signal in which significant change in certain statistical characteristics is unlikely to occur, but also detect any rapid changes in the interval if these statistical characteristics do vary. An algorithm to implement this test on a computer has been developed. In addition, this test will also detect the transition of the brain states and aid in extracting the dynamic properties of the process. We shall describe this test and its implementation and some preliminary results obtained by applying it to the EEG data furnished by NASA-Ames Research Center.

As proposed, we have also searched for other representations (transforms) of EEG signals which may furnish advantages over the Fourier transform. The Fourier spectrum is a signal representation in which the sinusoidal waveforms are used as basis functions. Different sets of basis functions will result in different spectra. The search for a new signal representation (transform) is tantamount to the quest for a new set of basis functions. In particular, we have used a set of orthonormalized square waves as basis functions to represent EEG signals. This set of square waveforms is known as the Walsh functions [3]. The resultant representation by using this set of square waveforms is thus called the Walsh transform. The Walsh transform is especially suitable for digital or digitized signals. The algorithm for Walsh transform is far faster than the fast-Fourier-transform, and it can be easily implemented by hardwire programming. Real-time computation of the Walsh spectra is a cinch. From our analysis of the EEG data furnished by NASA-Ames Research Center, the Walsh spectra enhance certain features of the EEG signals. We shall describe our analysis of EEG signals by

the use of Walsh transform and demonstrate its advantages.

In the phase-uncertainty model of EEG signals [4], there is the characteristic parameter $\underline{b}$ which is the propagation speed of the variance used as a measure of the uncertainty of the phase. We believe that this parameter $\underline{b}$ will be a good measure for alertness. In order to obtain a time-varying $\underline{b}$ from the EEG signals, we have used a sliding window and an estimator method rather than the correlation technique. The ultimate goal is to find a scalar relationship between the time-varying $\underline{b}$ and behavioral alertness measurements. It is essential to have a linear-phase filter so that the phase information in EEG will not be distorted after filtering. The previously used time-domain transversal filter does serve the purpose; however, it is extremely slow. We have implemented a frequency-domain linear-phase filter which operates in real time. The details of this filter will be described.

II. A Test for Stationarity in EEG Signals

To treat EEG signals as nonstationary processes, many researchers have used the short-time spectral analysis. This technique depends on the validity of the assumption that the signal remains at least wide-sense stationary in the interval when the short-time power density spectrum is being computed. For a process to be wide-sense stationary, its mean must be a constant and its autocorrelation function must be a function of the lagging interval alone. We have devised a sensitive method for detecting any changes of the stationarity conditions in the signal process for any intervals of time. The approach is to subject the mean and mean square of the signal process to randomness statistical tests in order to identify non-random variations of the parameters of interest in the course of time. This method will not only determine the epoch within which the signal process remains stationary but also will detect the transition of the brain states and thus will aid in extracting the dynamic properties of the process.

The mean, variance, and mean square are calculated for each successive one-second segment of data. These parameters then form a set of arrays consisting of from 5 to 25 elements. Each array then is composed of statistics representing an interval of data from 5 to 25 seconds, all intervals starting at the same reference as shown below:

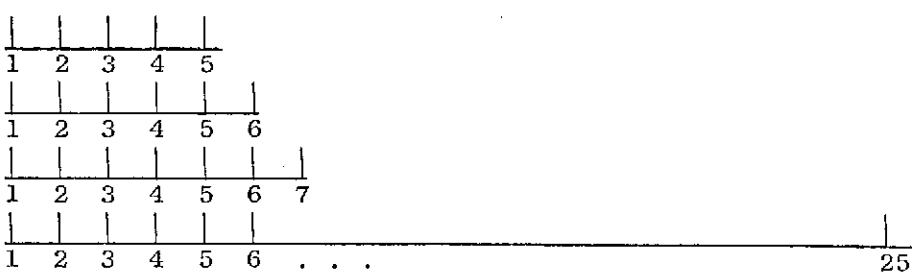

Each of these arrays is then subjected to four tests of nonrandomness, since each test is sensitive to a different type of trend. The four tests are:

a) Run test

b) Trend test

c) Mean Square Successive Differences test, and

d) Serial Correlation test.

Each test assigns a parameter value to each array. The parameter values are then plotted versus interval length, and trends are displayed. If there is a nonstationary trend, it will manifest itself by a significant change in one or more of the test parameters. The procedure is block diagrammed in Figure 1.

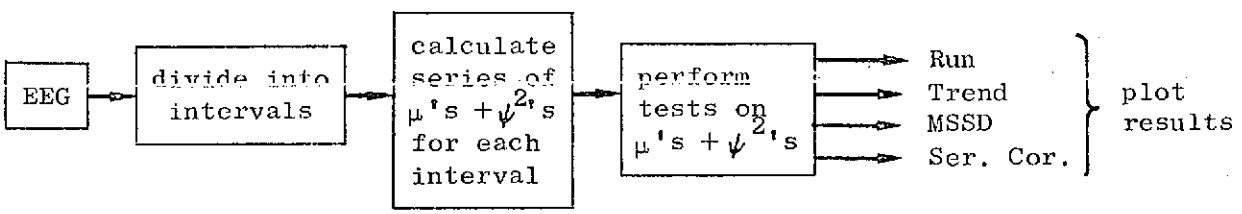

Figure 1 Block diagram for tests of nonstationarity

As an illustration, we have used the EEG data recorded while the human subjects with eyes closed were stimulated by stroboscopic flashes at the rate of 10 flashes per second for 50 seconds, then no stimulation for 50 seconds, then another 50 seconds of stimulation, etc. The EEG data were furnished by Dr. J. Anliker of NASA-Ames Research Center.

In this case the Mean Square Successive Differences test was the most sensitive to the state of strobe--on or off. It showed a change in test parameter starting shortly after the change in strobe status, and lasting several seconds. This corresponds to expected latency

periods for photically stimulated subjects.

Results

Figures 2 - 8 illustrate the effect of the strobe turning off. At the point marked T on the horizontal axis (e.g., 25 seconds in Figure 2), the strobe went off. This means (for Figure 2) the strobe was on for 25 seconds following the reference time. In Figure 3 the reference time in the EEG data is 6.3 seconds later than in Figure 2, and, therefore, the T indicating strobe off occurs after 18.7 seconds (25 - 6.3). In other words, the different figures represent the results of sliding a 25-second window along the EEG data with 6.3-second increments.

The dependent variable is the result of the Mean Square Successive Differences test run on the mean (μ), variance (σ^2) and mean square (ψ^2) for each interval from 5 to 25 seconds. Thus, in Figure 3 the first 14 points plotted (intervals 5 - 18) represent strobed data, and the last seven are combinations of pre- and post-strobed terminations.

As can be seen, there is no trend before T in all figures (which is reasonable since all the points represent strobed data). Starting with Figure 3 a trend can be seen beginning approximately one second after the cessation of strobing, and continuing for approximately 6 or 7 seconds. This is best seen in Figure 6. Figure 5 is a repeat of Figure 4 with polynomial regression lines (4th order) fit to the data. Examining this series of figures we observe that the effect of turning off the strobe is detected, and the nonstationary interval following this event is identified.

Figures 7 and 8 show the results of MSSD test for stimulus-off EEG signals where no trends have been detected.

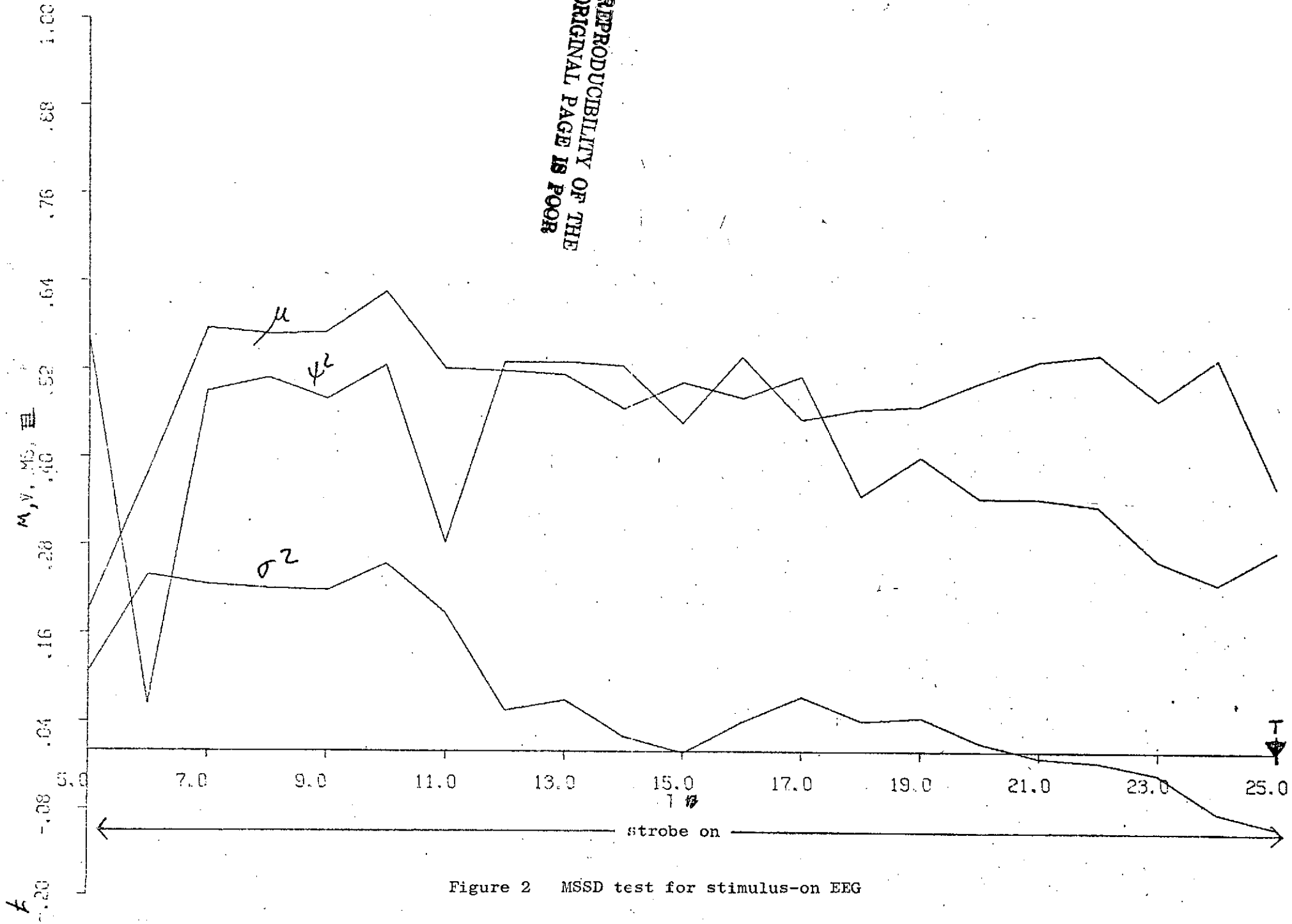

Figure 2 MSSD test for stimulus-on EEG

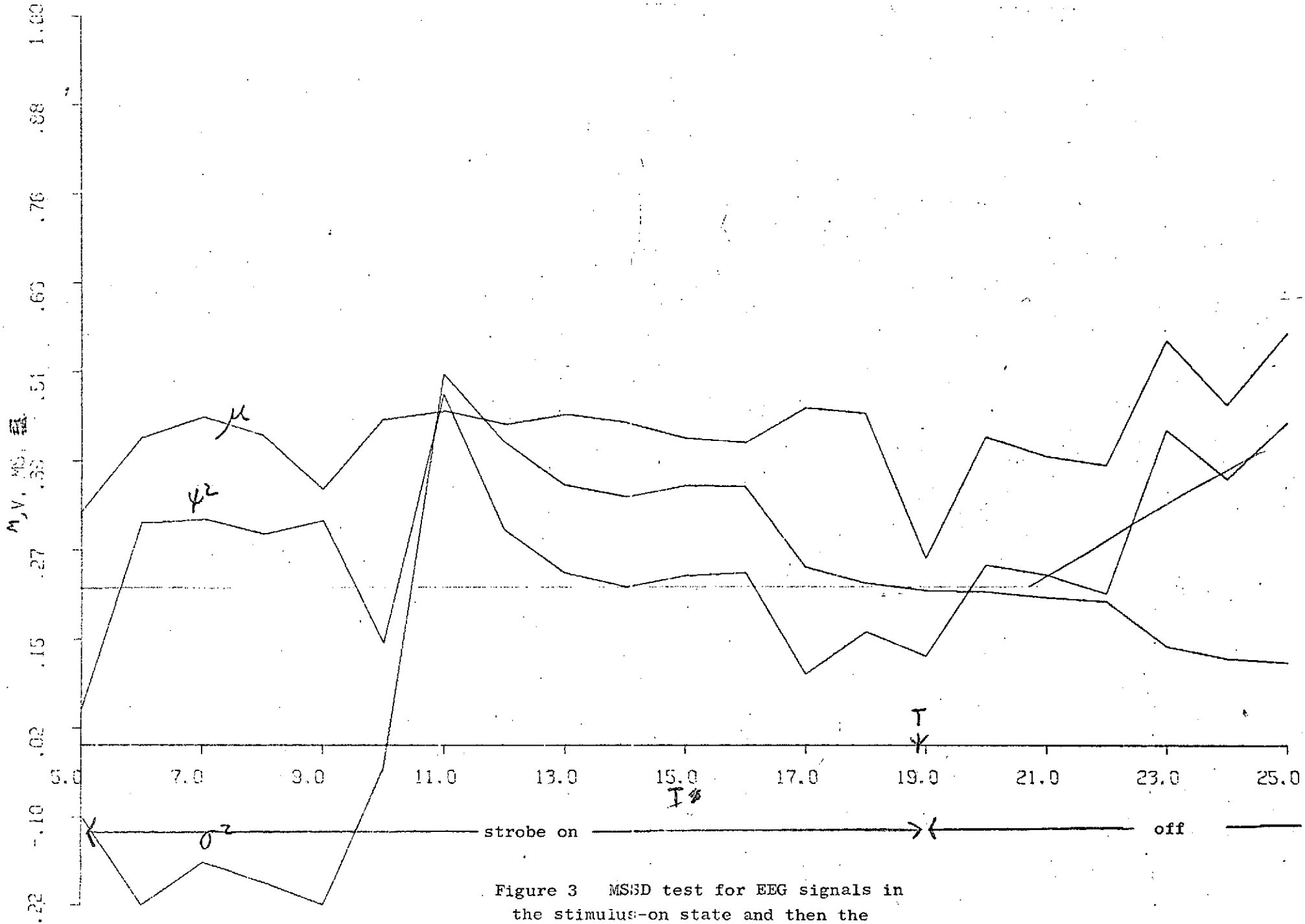

Figure 3 MSSD test for EEG signals in the stimulus-on state and then the stimulus-off state

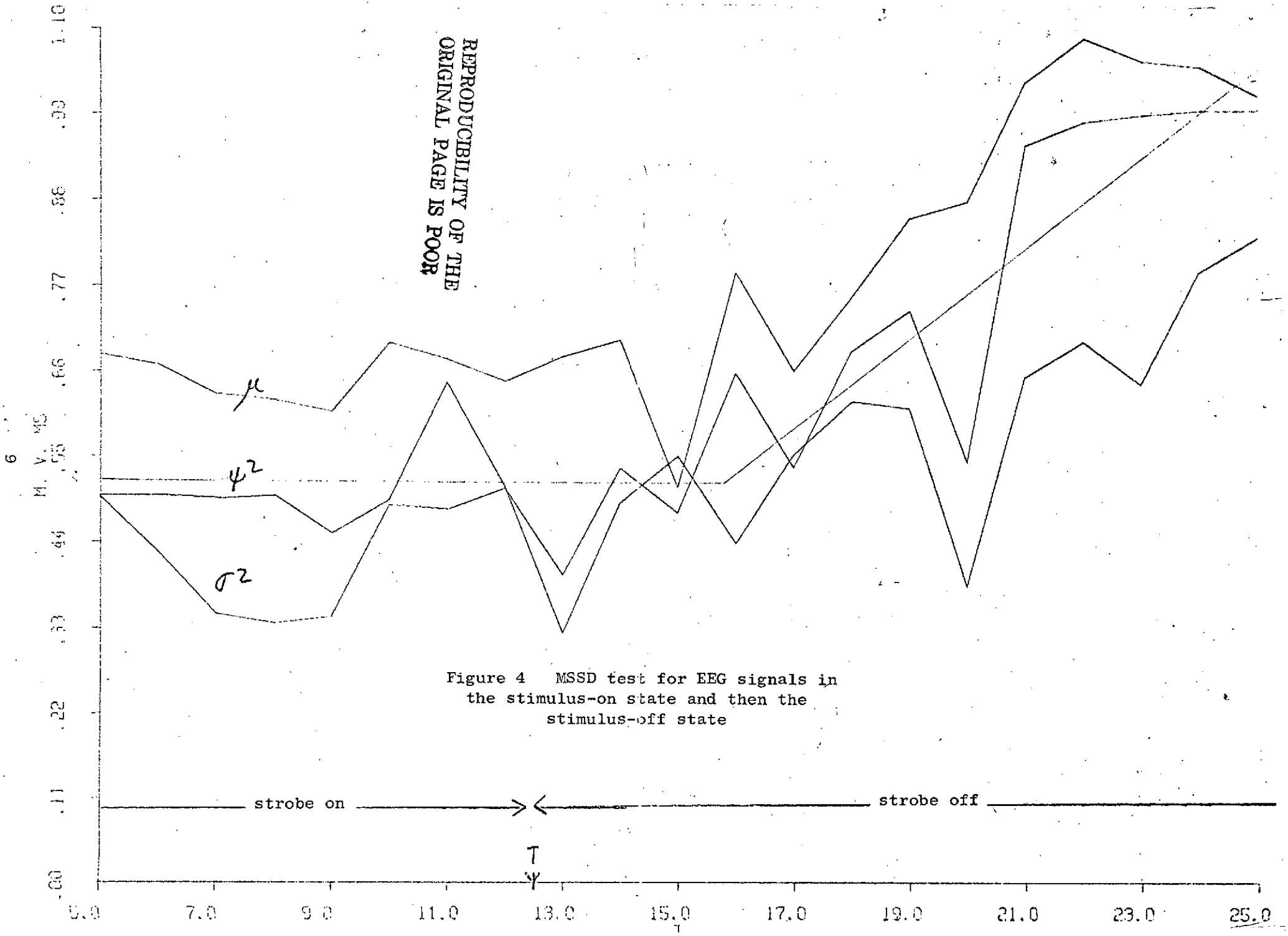

Figure 4 MSSD test for EEG signals in the stimulus-on state and then the stimulus-off state

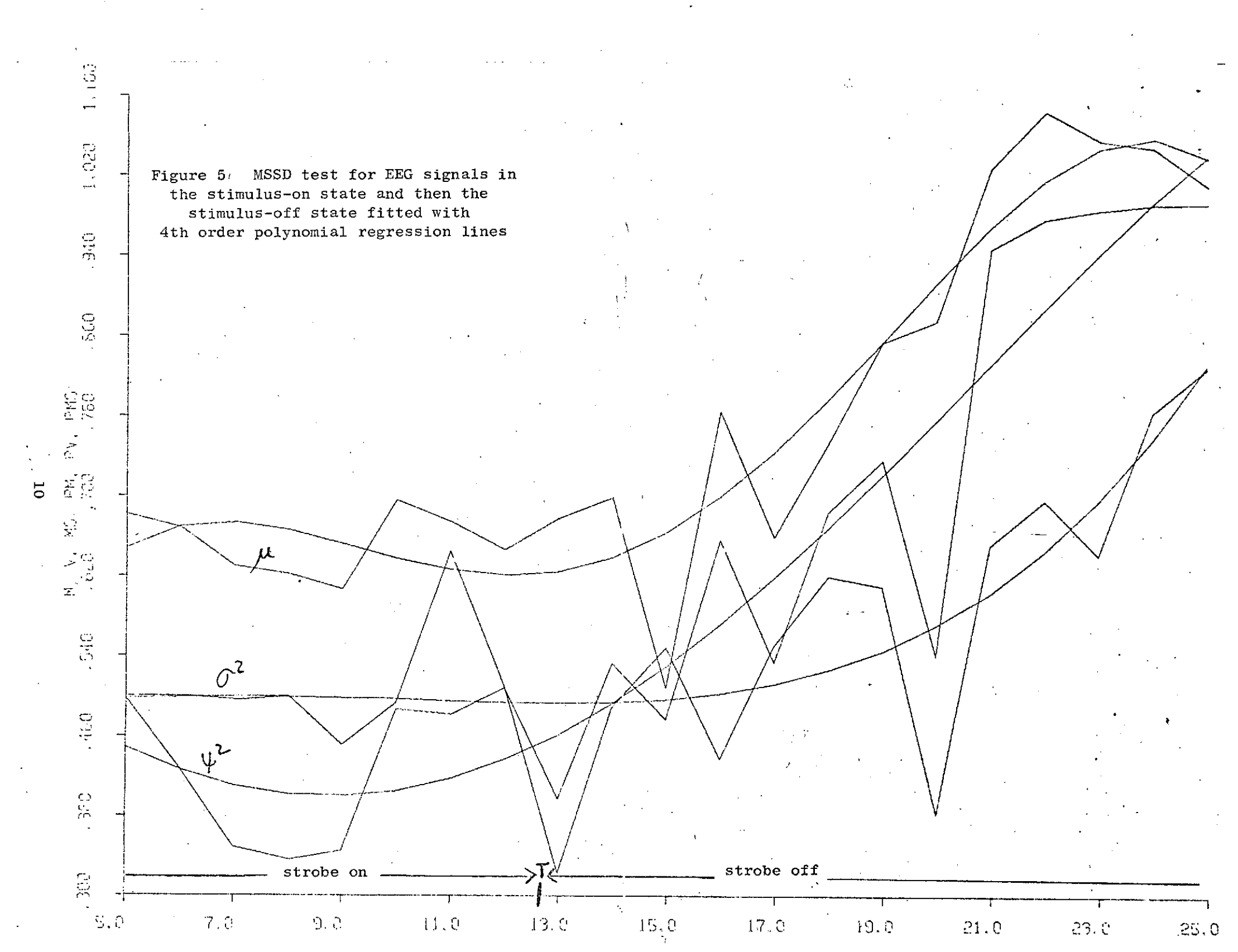
Figure 5. MSSD test for EEG signals in the stimulus-on state and then the stimulus-off state fitted with 4th order polynomial regression lines
μ
σ²
ψ²
strobe on
strobe off
T
5.0
7.0
9.0
11.0
13.0
15.0
17.0
19.0
21.0
23.0
25.0

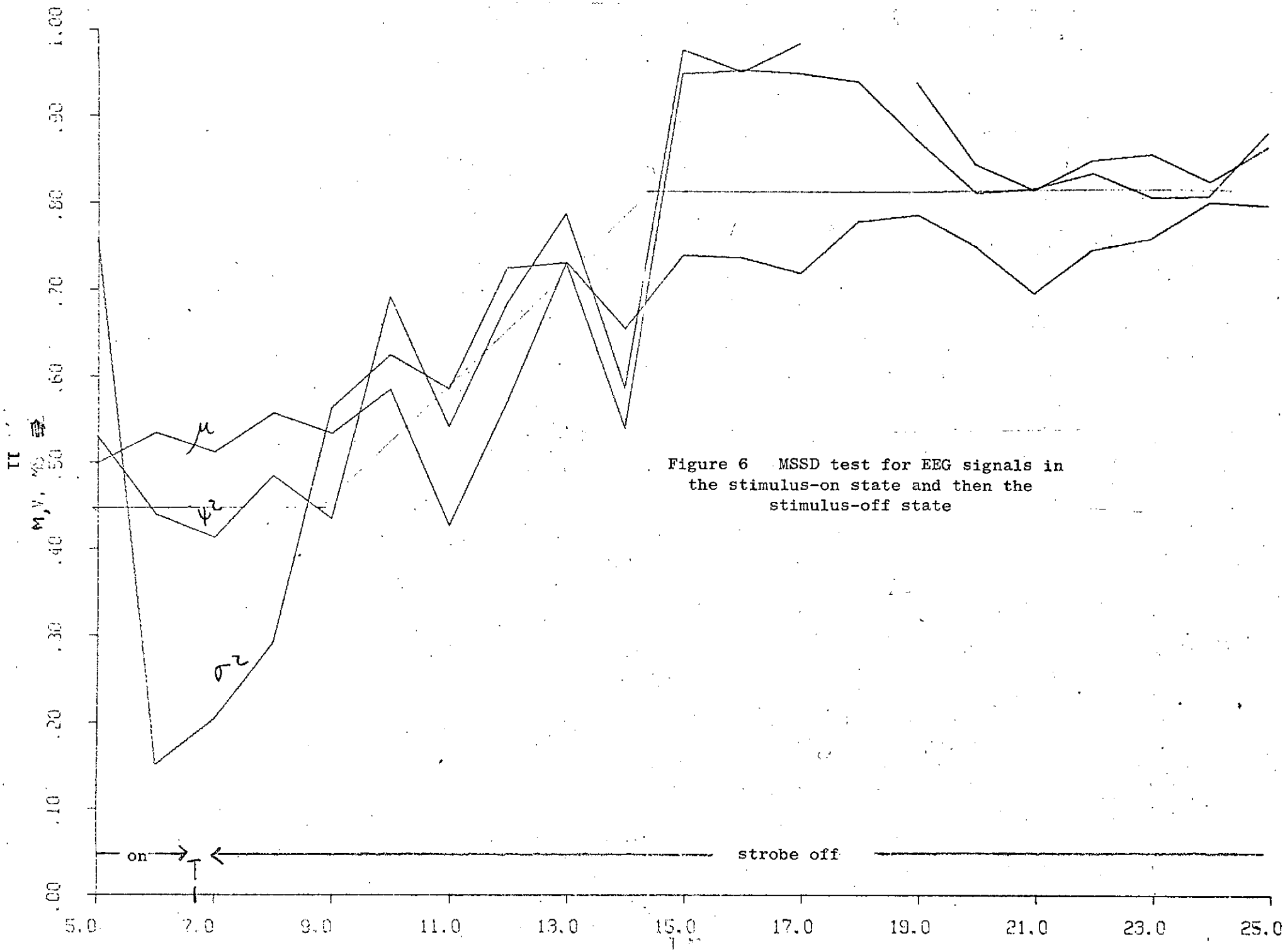

Figure 6 MSSD test for EEG signals in the stimulus-on state and then the stimulus-off state

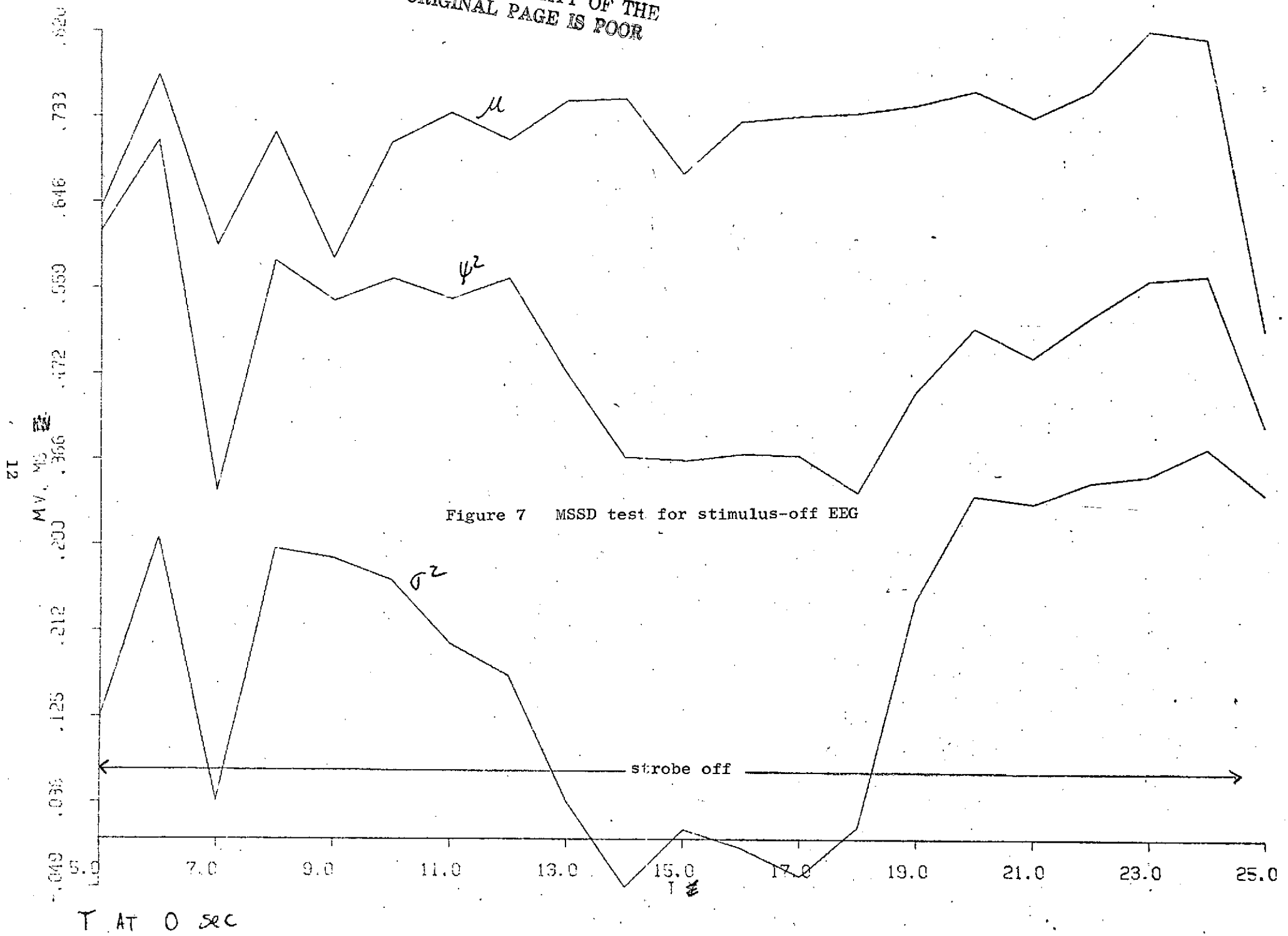

Figure 7 MSSD test for stimulus-off EEG

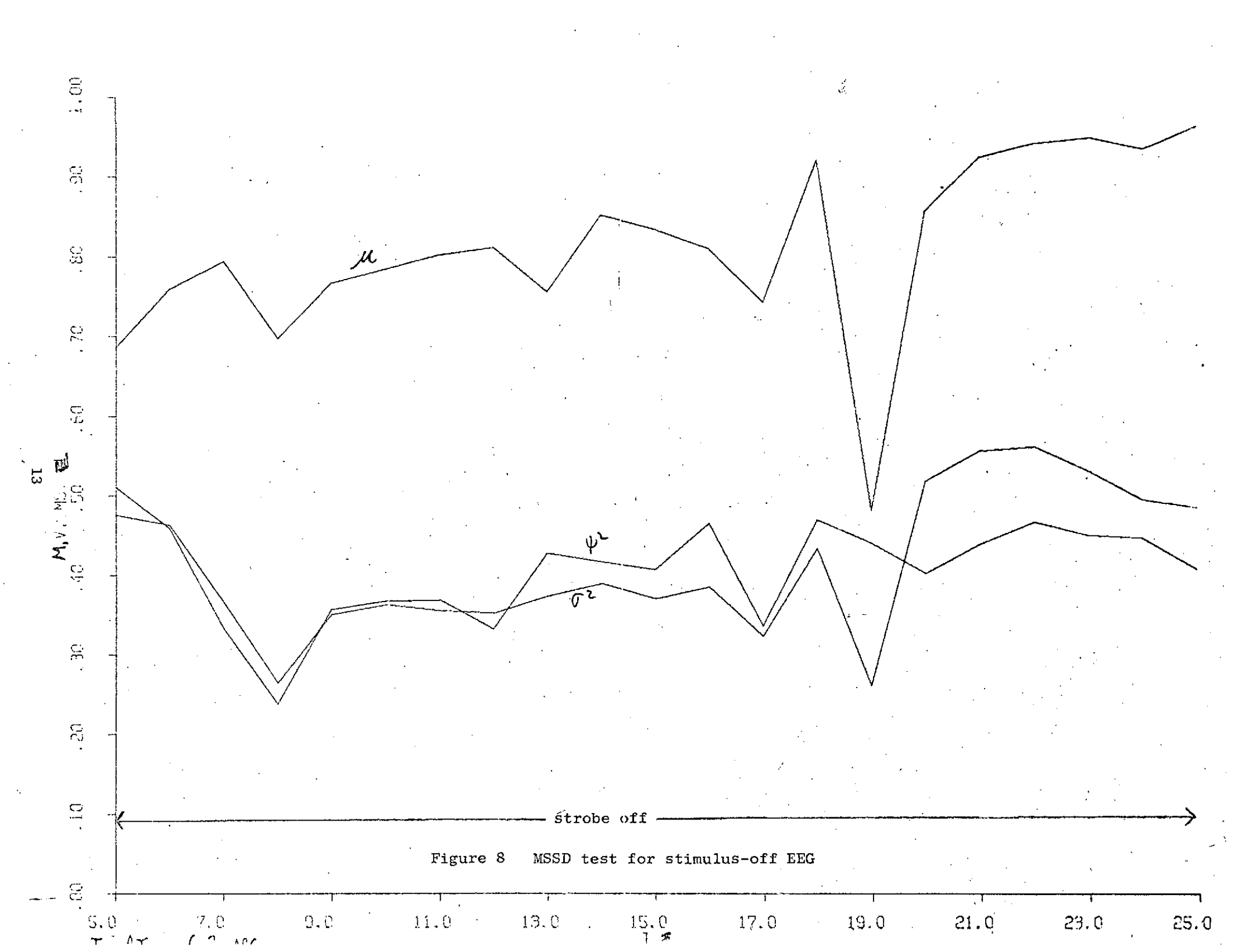

Figure 8 MSSD test for stimulus-off EEG

III. Representations of EEG Signals

In our search for new representations of EEG signals, we aimed at the efficiency of the representations and their enhancement of various desired features of the signal. The Karhunen-Loéve expansion offers the most efficient representation; however, it suffers from its difficulty in implementation. Fourier transform has proven to be useful in some EEG analysis. In the course of our work, we have developed and implemented a statistical representation in terms of amplitude, frequency, and phase of EEG signals [5] and the representation in terms of in-phase and quadrature components [6]; we have also looked into the Karhunen-Loéve expansion as discussed in the previous reports. The Walsh transform of EEG signals offers potentials not only in its efficiency of representation but also in its enhancement of certain desirable features of EEG signals. The Walsh transform is a representation in terms of a set of Walsh functions which were originally developed by J. Walsh in 1923 [3] and gained populatiry since 1968 [7]. Preliminary results showed that the Walsh spectra of EEG in the various sequency bands gave a better indication of the alertness states.

The representation of a signal $x(t)$ in terms of the set of Walsh functions is given by

$$x(t) = \sum_{k=0}^{\infty} W_k \, \mathrm{wal}\left(k, \frac{t}{T}\right), \quad 0 \le t \le T$$

where k is the number of zero crossings of Walsh functions. Lackey [8] presented a good review of the construction of Walsh functions from products of the incomplete, but simpler set of Radamacher functions. The Walsh coefficients are obtained by

$$W_k = \frac{1}{T} \int_0^T x(t) \text{ wal} \left(k, \frac{t}{T} \right) dt \quad .$$

For a digital (or discrete-time) signal which consists of N sampled data points, we may represent the elements of the digital signal by

$$x(m) = \sum_{k=0}^{N-1} W_k \text{ wal } (m,k) \quad , \; m = 0, 1, 2, \ldots, N-1$$

The Walsh coefficients are then given by

$$W_k = \frac{1}{N} \sum_{m=0}^{N-1} x(m) \text{ wal } (m,k) \; , \; k = 0, 1, 2, \ldots, N-1$$

The N-tuple formed by Walsh coefficients in ascending order of the index k is called the sequency ordered discrete Walsh transform; i.e., $x = \left[W_0, W_1, \ldots, W_{N-1} \right]^T$. Using the property that the discrete Walsh function is symmetric with respect to its arguments; i.e., wal (k,m) = wal (m,k) , we can write the inverse Walsh transform as

$$x(k) = \frac{1}{N} \sum_{m=0}^{N-1} f(m) \text{ wal } (k,m) \; , \; k= 0, 1, 2, \ldots , N-1$$

where $x(k)$ is the k^{th} element of x . It is thus shown that the forward transform and the inverse transform have exactly the same operations. The Walsh transforms are implemented through the fast Walsh transform (FWT) algorithms.

Typically, FWT schemes exploit the structure of the FFT except that the role of

$$W_N = e^{j \frac{2\pi}{N}}$$

in the FFT [9] is replaced by -1 in the FWT. This makes FWT so much faster than the FFT. The FWT algorithm requires only addition

and subtraction. Notable algorithm for the computation of FWT has been described in [10].

There are some important differences between signals represented in the Walsh domain and those in the Fourier domain. First of all, the digital signal N-vector $\bar{x}$ is represented exactly by the first N Walsh functions. This means that sampled data of finite duration is also sequency limited. This is, of course, not true in the frequency-domain representation where a time-limited signal is not band limited.

One can obtain finite segments of a signal $x(t)$ by multiplying the signal by a "window function" $w(t)$; that is, $x_p(t) = x(t) \cdot w(t)$, where

$$w(t) = \begin{cases} 1, & 0 \le t \le T \\ 0, & t > T \end{cases}$$

so that

$$x_p(t) = \begin{cases} x(t), & 0 \le t \le T \\ 0, & t > T \end{cases}$$

Now, let the Fourier transform of $x(t)$ be $X(f)$; i.e.,

$$F[x(t)] = X(f), \text{ then } F[x(t) \cdot w(t)] = X(f) * W(f)$$

where

$$W(f) = K \frac{\sin af}{af} \quad ;$$

and $\underline{K}$ and $\underline{a}$ are constants; and $*$ denotes convolution. This result shows that the Fourier transform is distorted through the convolution with the frequency-domain window function. It is well known that the error may be minimized by applying a corrective weighting function such as Hamming window. This extra processing is used solely to correct the distortion effects of the data windows. Such distortion does not

occur in the Walsh domain because the window function is one of the basis functions; namely, $w(t) = \text{wal}\ (0,t)$. This is easily seen by the following reasoning: Taking the same data window $w(t)$, we obtain for the finite segment of the signal $x(t)$ as

$$x(t) \cdot w(t) = \sum_{k=0}^{\infty} W_k \ \text{wal}\ (k,t) \cdot \text{wal}\ (0,t) \quad .$$

Since the complete set of Walsh functions is closed in multiplication and $\text{wal}(k,t) \cdot \text{wal}\ (m,t) = \text{wal}\ (k \oplus m, t)$ where $\oplus$ denotes module 2 addition with no carry; i.e.,

$$1 \oplus 0 = 1$$
$$1 \oplus 1 = 0$$
$$0 \oplus 0 = 0 \quad ,$$

$\text{wal}\ (k,t) \cdot \text{wal}\ (0,t) = \text{wal}\ (k,t)$ and hence $x(t)\ w(t) = \sum_k W_k \ \text{wal}\ (k,t)$. It is clear that the window function $w(t)$ introduces no distortion at all in the Walsh domain.

In summary, the Walsh-domain representation has two distinct advantages over the Fourier-domain representation for discrete signals in addition to its computational speed. First, the data is exactly represented by a finite set of Walsh functions, and secondly, no distortion is introduced by the finite window function. Therefore, no correction such as the use of Hamiming or Hanning window is necessary.

We shall now turn our discussion to some properties of Walsh functions which we may utilize to our advantage. Let us consider a signal $f_1(t)$ which is periodic with period $2T$ and a signal $f_2(t)$ which is the same as $f_1(t)$ except that it has period T as shown in Figure 9. In other words, $f_2(t)$ is a time-compressed version of $f_1(t)$; i.e.,

$f_2(t) = f_1(2t)$, $t \geq 0$.

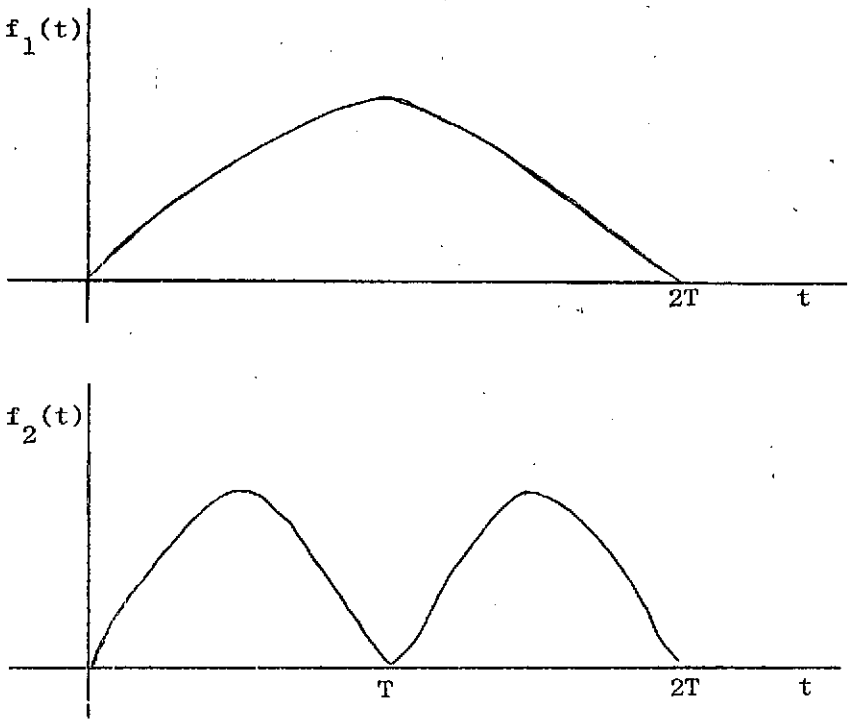

Figure 9 Time compression of a periodic signal

Representing the signals $f_1(t)$ and $f_2(t)$ in the Walsh domain, we obtain

$$f_1(t) = \sum_{k=0}^{\infty} W_k \text{ wal } (k,t)$$

and

$$f_2(t) = \sum_{k=0}^{\infty} W_k^1 \text{ wal } (k,t) \quad .$$

The time compression condition $f_2(t) = f_1(2t)$ implies that

$$\sum_{k=0}^{\infty} W_k^1 \text{ wal } (k,t) = \sum_{k=0}^{\infty} W_k \text{ wal } (k,2t) \quad .$$

From the definition of the Walsh functions, we have wal (k,2t) = wal (2k,t) ; hence,

$$\sum_{k=0}^{\infty} W_k^1 \text{ wal } (k,t) = \sum_{k=0}^{\infty} W_k \text{ wal } (2k,t) \quad .$$

Therefore,

$$W_0^1 = W_0$$

$$W_1^1 = 0$$

$$W_2^1 = W_1$$

$$W_3^1 = 0$$

$$W_4^1 = W_2$$

$$W_k^1 = W_{k/2} \quad , \quad k \text{ even}$$

$$W_k^1 = 0 \quad , \quad k \text{ odd}$$

For further compression in time such as $f_2(t) = f_1(mt)$, where $m = 2^{\ell}$, $\ell = 1, 2, \ldots,$ we obtain

$$W_k^1 = \begin{cases} W_{k/m} \ , \left[\frac{k}{m}\right] \text{ is an integer} \\ 0 \ , \text{ otherwise} \end{cases}$$

In essence, it says that compressing time by a power of 2 leaves the Walsh spectrum completely unaffected except for intervening zeros. This property may be used effectively for the detection of subharmonics in a signal. For example, we show the spectrum of a signal which has period T = 1.024 seconds in Figures 10 and 11. Figure 10 shows the spectrum without subperiods and Figure 11 shows that with 8 subperiods. Notice there are 8 intervening zeros in Figure 11.

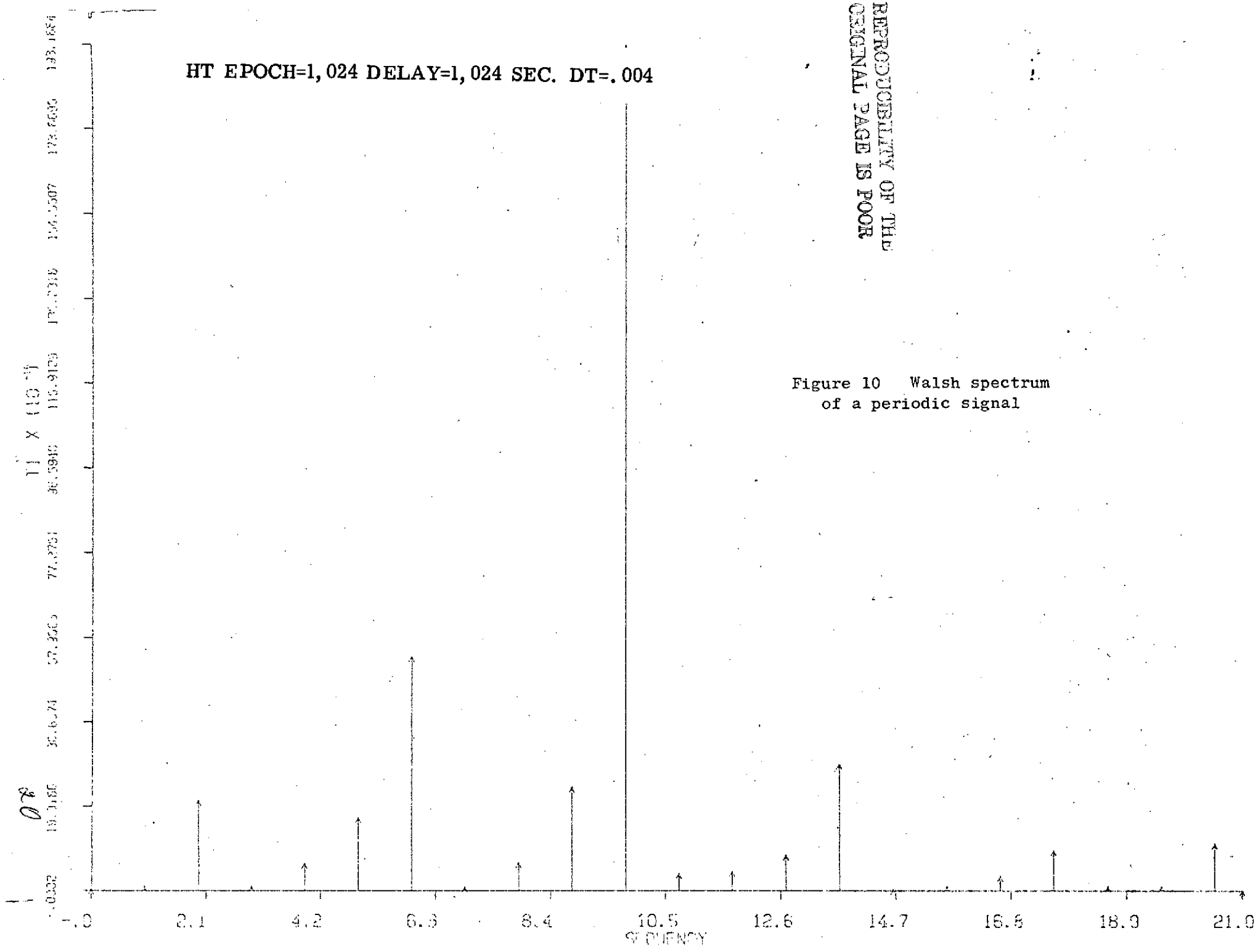

Figure 10 Walsh spectrum
of a periodic signal

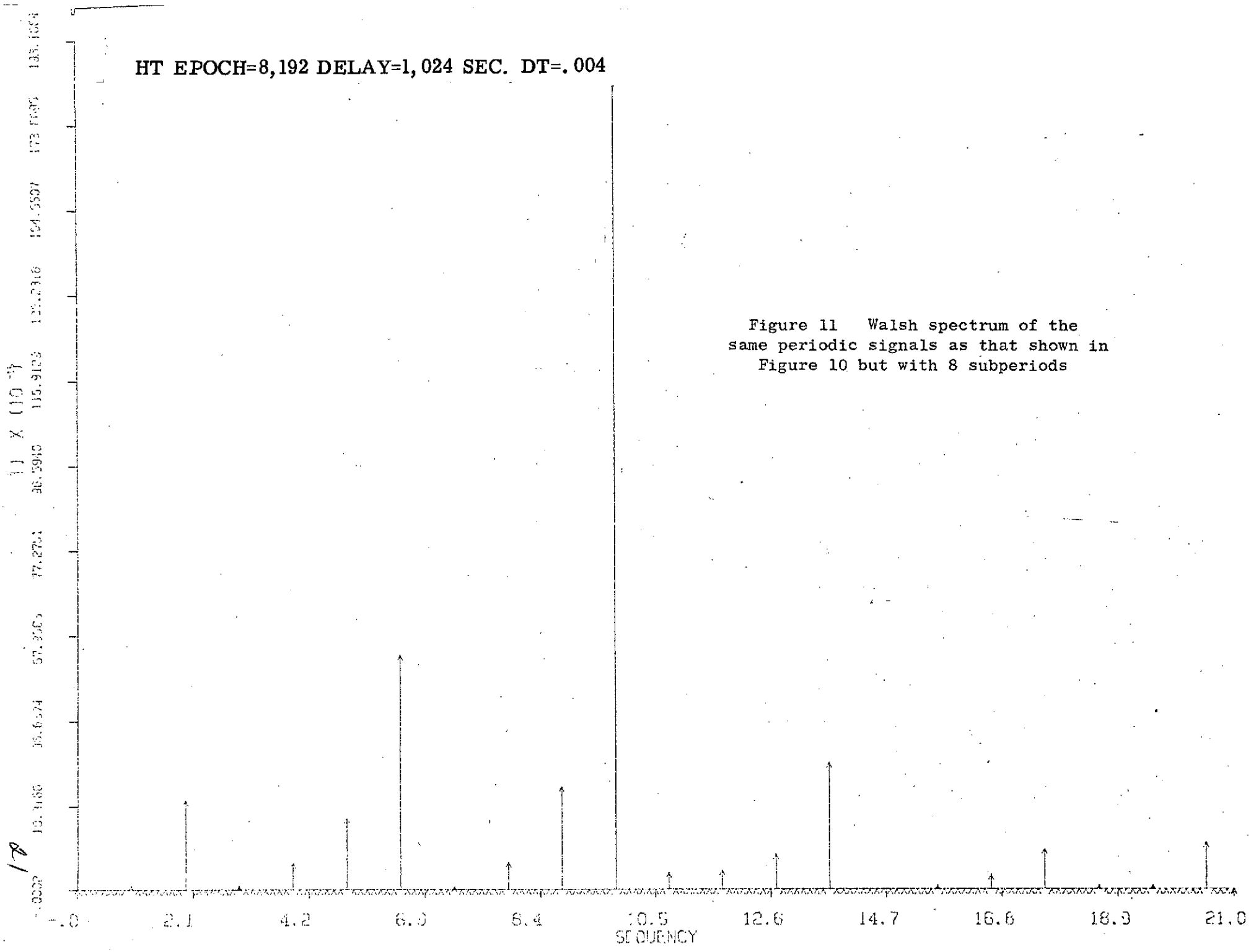

Figure 11 Walsh spectrum of the same periodic signals as that shown in Figure 10 but with 8 subperiods

The convergence property of the Walsh representation compares very favorably with the Fourier representation. To demonstrate, we computed the percentage loss in the signal energy (or the normalized mean squared error) of a section of EEG about 1 second in length for both the Fourier and Walsh transforms. The results are plotted in Figure 12. It is clear that the Walsh transform has a better convergence property than the Fourier transform in the lower range. In other words, in the range between 0 to 40 terms the Walsh transform requires fewer number of terms to achieve the same amount of mean-squared error as that required by the Fourier transform. Figure 13 shows a typical Walsh and Fourier spectra of a record of EEG signals. Some preliminary results have shown that the Walsh transform does enhance certain features of EEG signals. Further work is in progress for utilizing these features for EEG classification purposes.

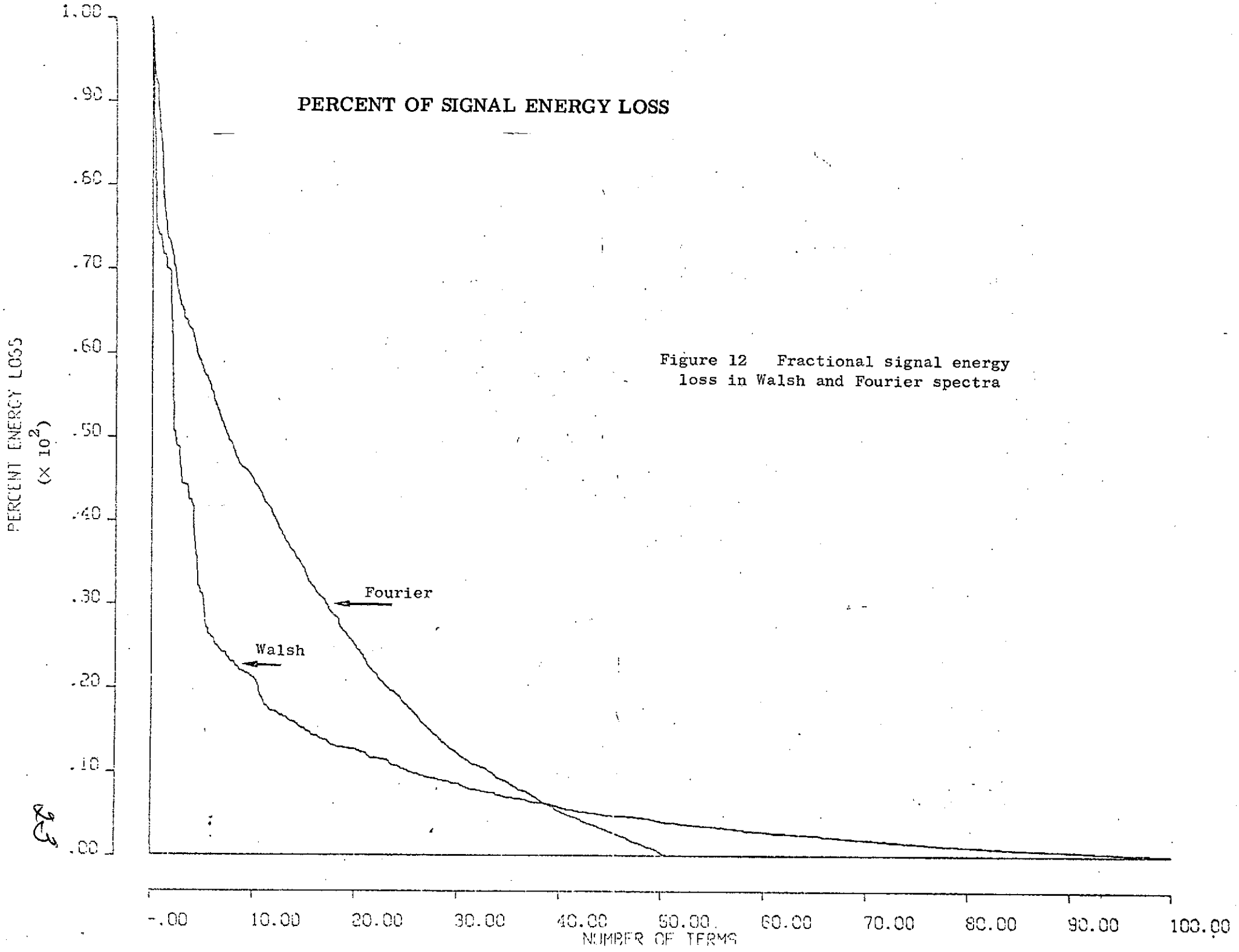

Figure 12 Fractional signal energy loss in Walsh and Fourier spectra

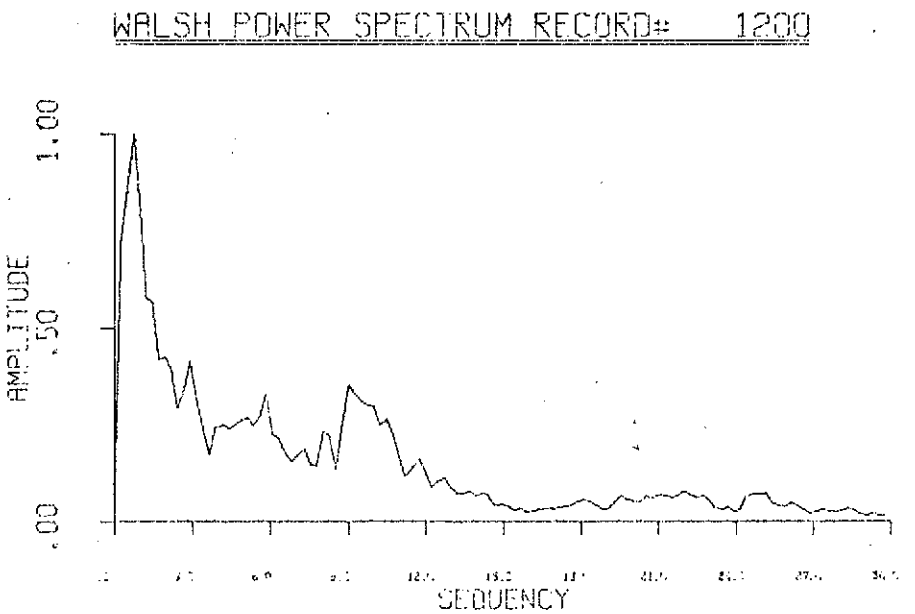

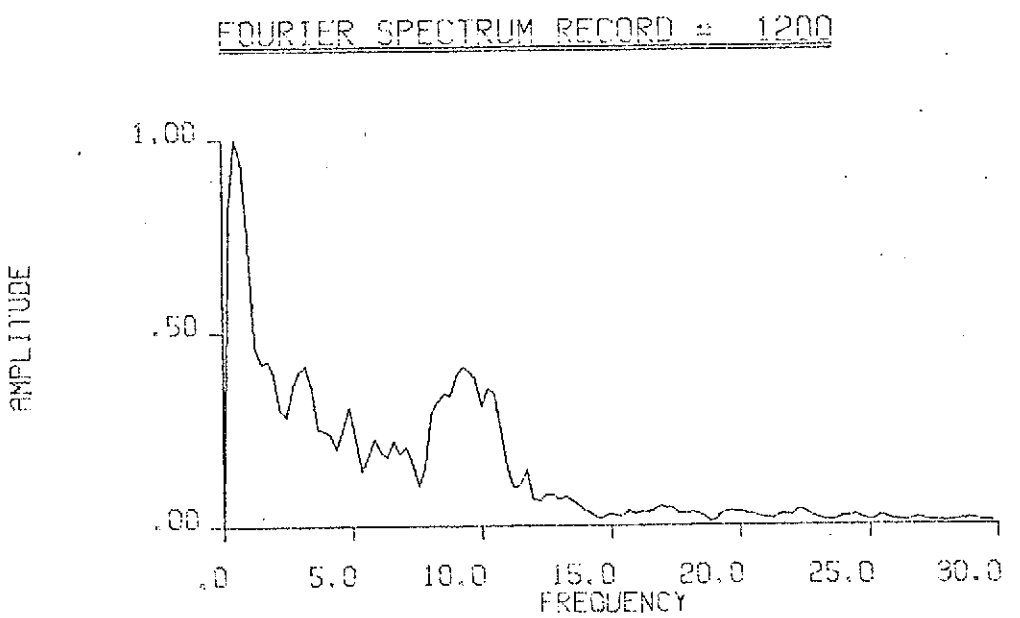

Figure 13 Walsh and Fourier spectra of an EEG signal

IV. A Digital Phase-Distortionless Filter Operating in the Frequency Domain

In phase uncertainty model for the EEG signals to extract the parameter b as a measurement of alertness, it is critical to filter the EEG signal by a phase-distortionless filter. Such a filter operating in the time domain was used in previous studies. Since this filtering requires that the EEG signal convolves with the finite duration impulse response of the filter, it is extremely slow. This, of course, prohibits real-time usage. A phase-distortionless filter must have linear-phase characteristics in the frequency domain. In order for a ditial filter to possess linear phase characteristics, the impulse response of its system function must satisfy the condition

$$h(n) = h(N - 1 - n) \quad .$$

This requirement is easily met in digital filtering. It results in a linear phase shift which corresponds to a delay of $(N-1)/2$ sample points. The input data $x(n)$ is first partitioned into data segments $x_k(n)$ of length M ; i.e.,

$$x_k(n) = \begin{cases} x(n) & , \ kM \leq n \leq (k+1)M-1 \\ 0 & , \ \text{otherwise} \end{cases}$$

Hence, $x(n)$ is simply the sum of the $x_k(n)$'s or

$$x(n) = \sum_{k=-\infty}^{\infty} x_k(n)$$

and the filtered output $y(n)$ is the result of convolution of the two sequences; i.e.,

$$y(n) = x(n) * h(n) = \sum_{k=-\infty}^{\infty} x_k(n) * h(n)$$

Each of the terms in the convolution sum is of length (N+M-1) where

N = filter length

M = data length .

For each output point, there are numerous multiplications and additions. The astronomical number of such operations renders this scheme extremely slow. In order to speed up the process, other means must be found. We decided to use the frequency-domain approach. From the above discussion, we found that to effect the convolution in the frequency domain, the transforms must be computed on a basis of at least (N+M-1) points. The (N-1) and (M-1) locations subsequent to the N^{th} filter coefficient and the M^{th} data point, are respectively filled with zeros before each transform is taken. Since the FFT results in a circular convolution of the two sequences, the desired output sequence is obtained by reconstructing the filtered sections in such a way that convolution is achieved. The filtered sections are simply the results of inverse transform of the sequence obtained by multiplying the transformed data sequence, term by term, with the transformed filter coefficient sequence. The procedure for reconstructing the filtered sections is referred to as the overlap-add method. This complete operation involves FFT and multiplications in one scope for obtaining the whole section of the filtered results; whereas the time-domain operation requires multiplications and additions for each ouput point.

Moreover, additional savings in time could be achieved by this frequency-domain operated filtering procedure if both of the signal and filter sequences are real. In general, the filtered sections $y_k(n)$ are

complex; i.e.,

$$\begin{aligned} y_k(n) &= \mathrm{Re}\left[y_k(n)\right] + j\mathrm{Im}\left[y_k(n)\right] \\ &= \mathrm{Re}\left[x_k(n)\right] * \mathrm{Re}\left[h(n)\right] - \mathrm{Im}\left[x_k(n)\right] * \mathrm{Im}\left[h(n)\right] \\ &\quad + j\left\{\mathrm{Im}\left[x_k(n)\right] * \mathrm{Re}\left[h(n)\right] + \mathrm{Re}\left[x_k(n)\right] * \mathrm{Im}\left[h(n)\right]\right\} . \end{aligned}$$

Our filter is real; hence,

$$\mathrm{Im}\left[h(n)\right] = 0$$

and $y_k(n)$ becomes

$$y_k(n) = \mathrm{Re}\left[x_k(n)\right] * \mathrm{Re}\left[h(n)\right] + j\left\{\mathrm{Im}\ x_k(n) * \mathrm{Re}\left[h(n)\right]\right\} .$$

If the data sequence is also real, two separate convolutions with the same kernel sequence can be performed simultaneously. Therefore, when convolving real signals with real impulse responses, the FFT is capable of double performance. This is achieved by loading the data in both the real and imaginary parts of the data sequence to be transformed and processed with the same impulse response of the filter. Thus, we are able to save additional time in the filtering process. The double-performance overlap-add method is depicted in Figure 14 in which section a is discarded, as it constitutes the inherent delay. The subsequent sections in Figure 14 are dealt with in the following manner: Unprimed and primed sections are added together term by term and the continuous filtered output is obtained by stringing together the resultant sections.

A few words about the judicious choice of the data length M and the filter impulse response length N are in order. There are two major considerations: (a) N must be sufficiently large so that the ratio of the Hamming weighted impulse response side-lobe width to the

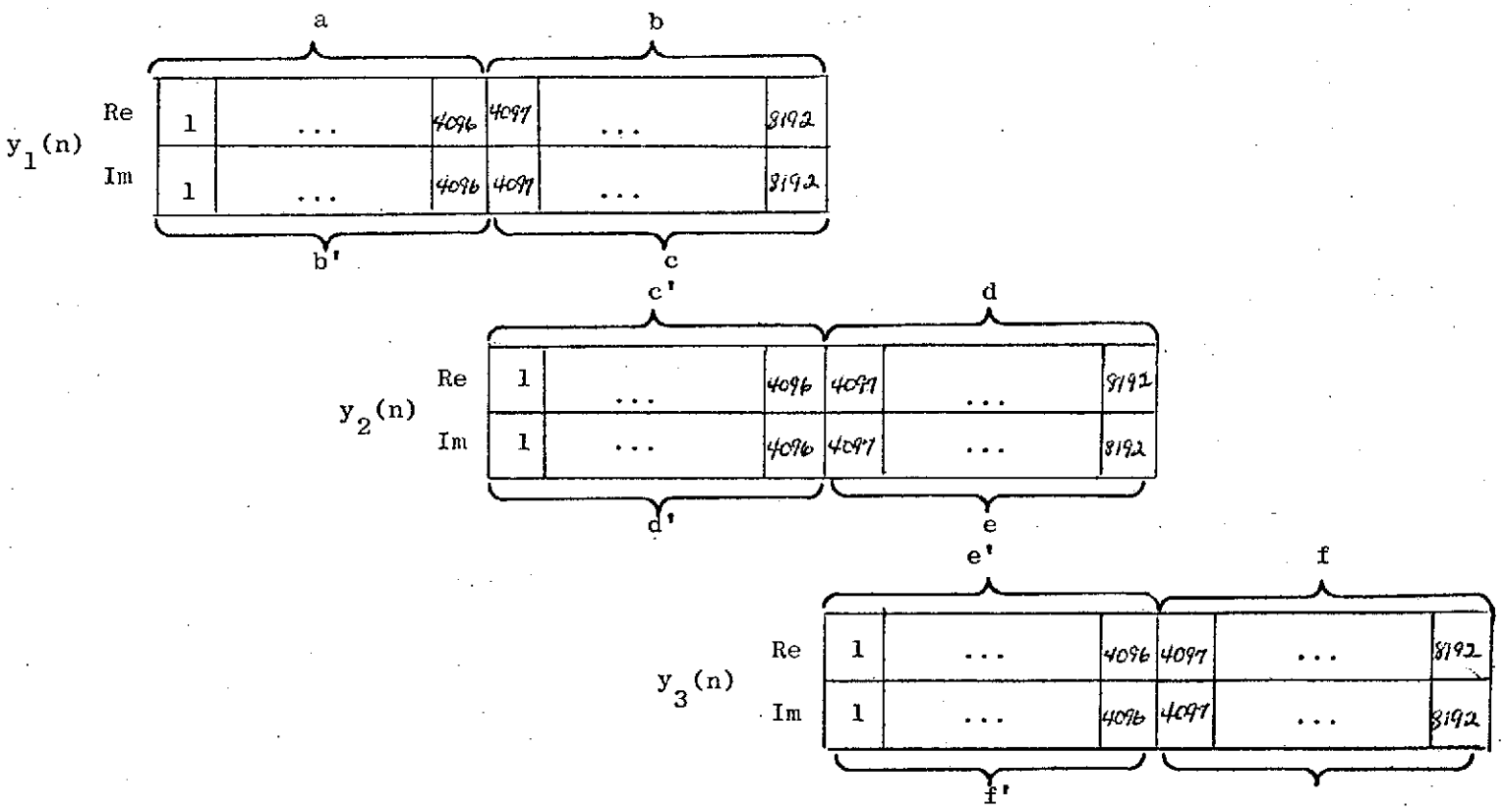

Figure 14 Double-performance overlap-add method

main-lobe width is sufficiently small in order to achieve a sharp cutoff in the frequency response characteristic; (b) The overlap-add procedure described previously will be more efficient computationally when $N = M + 1$ and $N + M - 1 = 2^i$, where i is an integer. In our application, we chose $N = 4097$ and $M = 4096$. This choice does satisfy the above considerations. The frequency-domain operated phase distortionless digital filter which we have designed and used has a passband of 8 to 13 Hz. Its amplitude response characteristic is shown in Figure 15. Notice the sharp cutoff feature of this filter. We show the flowchart of this filter in Figure 16, and the resultant filtered output of a section of EEG signal by the use of frequency-

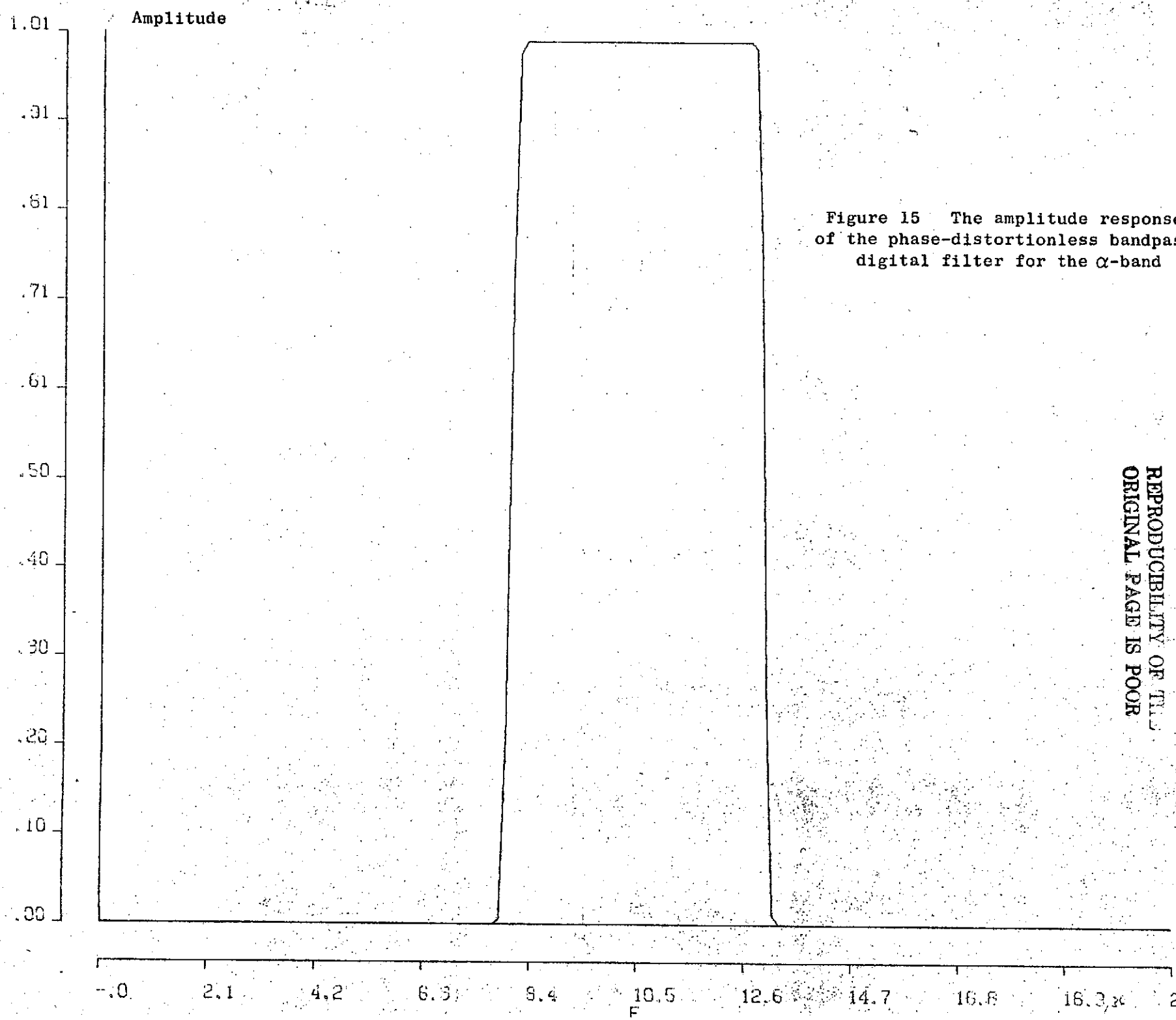

Figure 15 The amplitude response of the phase-distortionless bandpass digital filter for the α-band

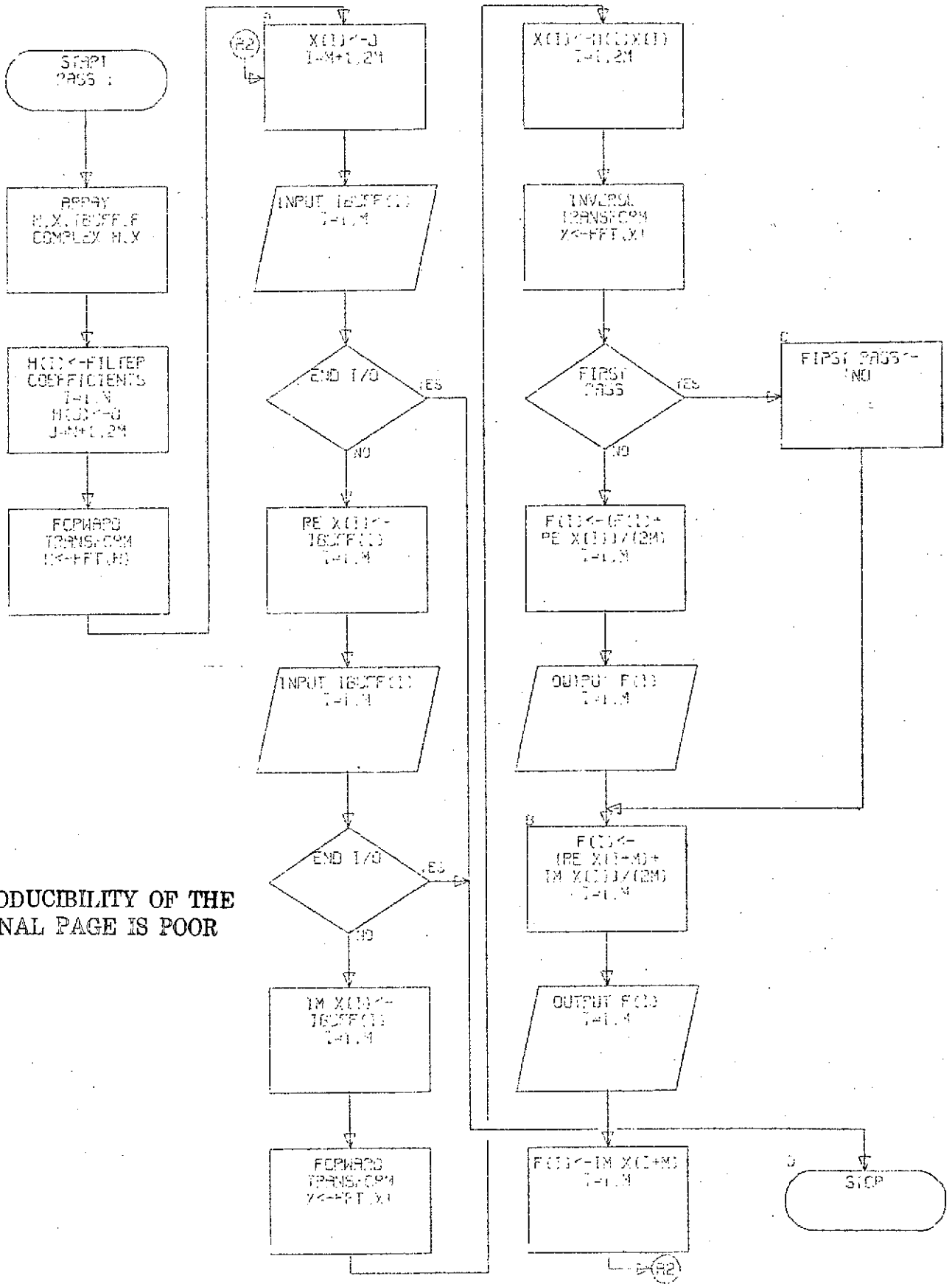

Figure 16 Flowchart of the phase-distortionless digital filter

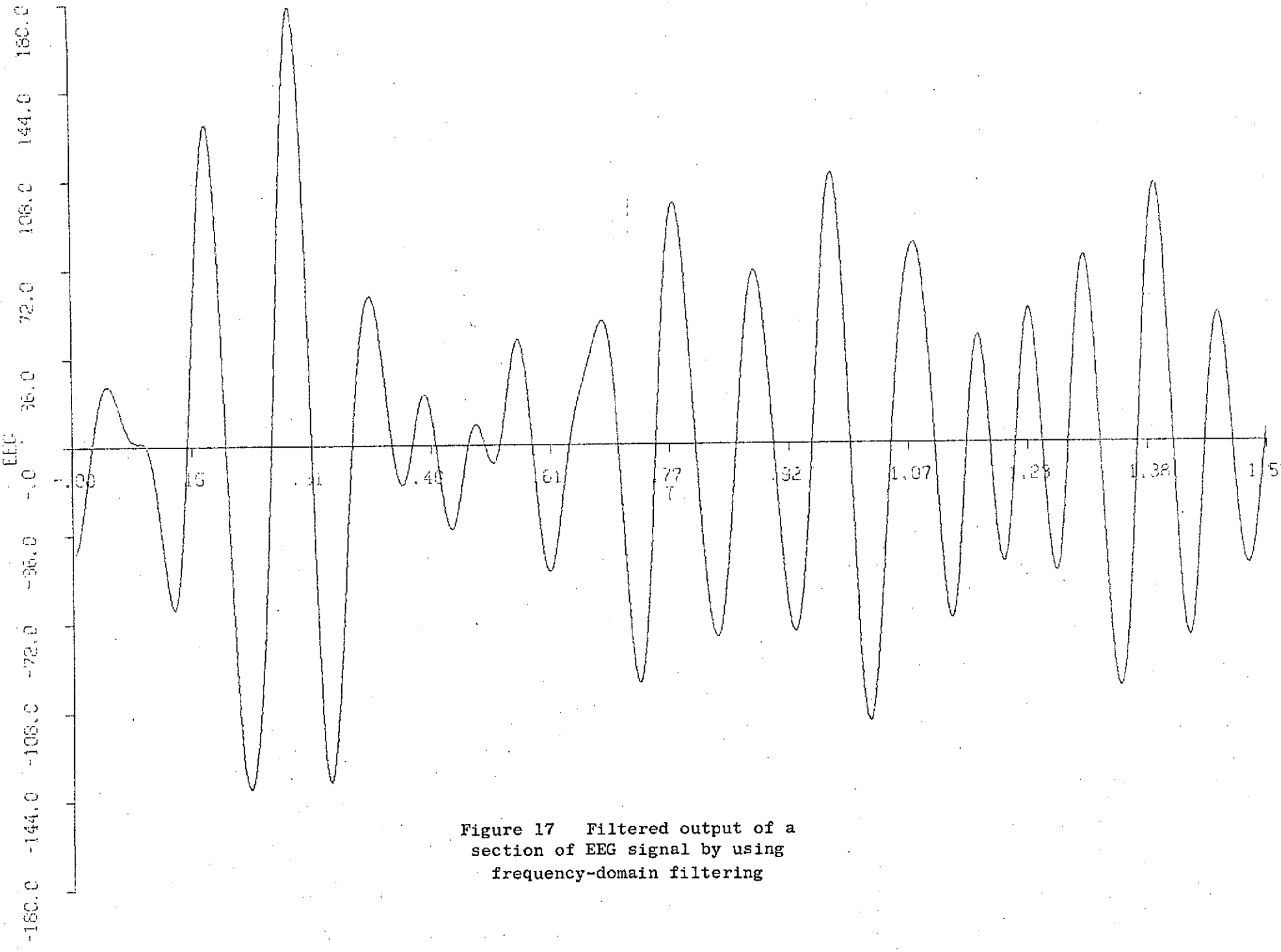

Figure 17 Filtered output of a section of EEG signal by using frequency-domain filtering

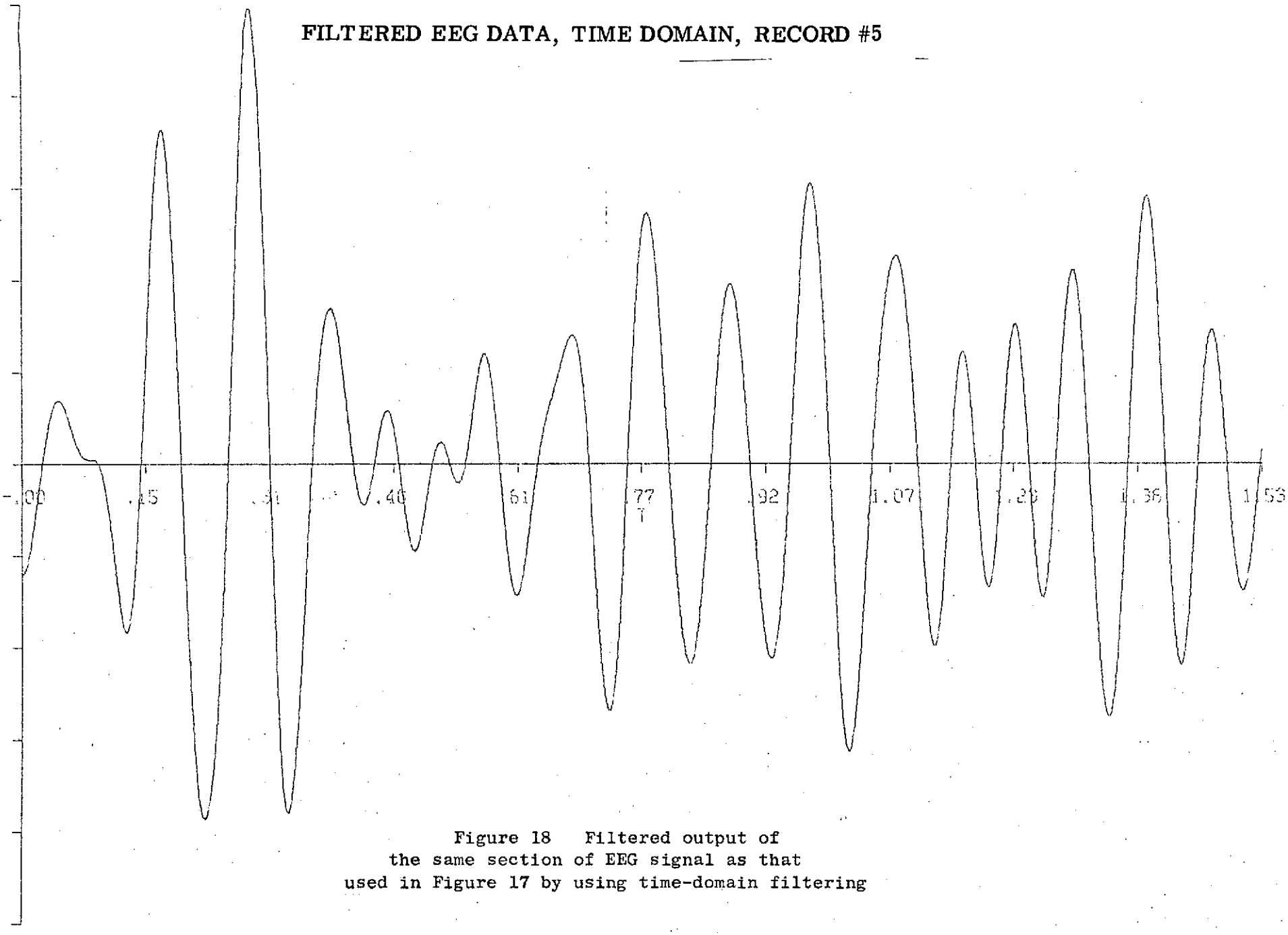

Figure 18 Filtered output of
the same section of EEG signal as that
used in Figure 17 by using time-domain filtering

domain filtering in Figure 18. From these figures we observe that the resultant outputs are identical.

From previous discussion, we may conclude that the phase-distortionless filtering in the frequency domain is versatile and faster than the time-domain filtering. The use of FFT permits the filtering to be accomplished on real-time basis; whereas the time-domain filtering for the same length of data will take at least fifty times longer to accomplish. In other words, the frequency-domain filtering needs only 1/50 of the time needed for the time-domain filtering. Besides, the FFT is also capable of double performance discussed previously. We may use this double-duty feature to filter simultaneously either two independent channels of EEG signals or one channel of EEG signals in two different bands of interest.

V. Conclusion

The work has been progressing along the lines as proposed. Our preliminary results presented in this report show great promise. The tests for stationarity in EEG signals are designed for the determination of the length of signal interval in which spectral analysis is valid and have great potential in extracting the dynamic characteristics of the signal process. This will, undoubtedly, help in the detection of changing states of alertness. In the area of searching for new representation, we described the use of Walsh transform and showed its advantages. In the modeling of EEG signals, we described in detail the phase-distortionless digital filter in the frequency domain. Its versatility and speed have been proven from our results. This filter can be operated in real time in contrast to the time-domain filtering techniqued used previously which is fifty times slower. Without question, this filtering technique will speed up the estimate of the parameter $\underline{b}$ in the model for alertness measure.

References

[1] Kawabata, N., "A nonstationary analysis of the electroencephalogram", IEEE Trans., Vol. BME-20, No. 6, pp. 444-452, November 1973.

[2] Anliker, J. E., Friedlander, S., Mansfield, F., and Finger, H., "Nonstationary processes in the electroencephalogram during sleep", Proc. of the 27th Annual Conference on Engineering in Medicine and Biology, p. 145, October 1974.

[3] Walsh, J. L., "A closed set of orthogonal functions", Am. J. Math., Vol, 55, pp. 5-24, January, 1923.

[4] Floyd, R. V., Lai, D. C., and Anliker, J. E., "A model for the photically stimulated electroencephalograhic signals", Proc. of the San Diego Biomedical Symposium, Vol. 12, pp. 5-16, 1973.

[5] Lux, R., "A statistical representation of the alpha rhythm in the human EEG with applications to the classification and prediction of behavior states", Ph.D. Thesis, University of Vermont, May, 1974.

[6] Ein-Gal, M. and Lai, D. C., "Real-time EEG analysis and monitoring using in-phase and quadrature components", Proc. of the 26th Annual Conference in Medicine and Biology, p. 401, 1973.

[7] Harmuth, H. F., "A generalized concept of frequency and some applications", IEEE Transactions on Information Theory, Vol. IT-14, No. 3, pp. 375-382, May 1968.

[8] Lackey, R. B., and Meltzer, D., "A simplified definition of Walsh functions", IEEE Transactions on Computers, pp. 211-213, February, 1971.

[9] Ulman, L. J., "Computation of the Hadamard transform and the R transform in ordered form", IEEE Transactions on Computers, pp. 359-360, April, 1970.

[10] Shanks, J. L., "Computation of the fast Walsh-Fourier transform", IEEE Transactions on Computers, pp. 457-459, May, 1969.